Preparation, Structure Determination, and Redox Characteristics of New Calcium Copper Phosphates

B. I. Lazoryak,*,[1] N. Khan,* V. A. Morozov,* A. A. Belik,* and S. S. Khasanov†

Chemical Department, Moscow State University, 119899 Moscow, Russia; and †Institute of Solid State Physics, 142452, Chernogolovka, Russia
E-mail: lazoryak@ctech.chem.msu.su

New calcium copper phosphates o-$Ca_{19}Cu_2(PO_4)_{14}$, r′-$Ca_{19}Cu_2H_{1.42}(PO_4)_{14}$, and r″-$Ca_{19}Cu_{2-y}H_{2.24}(PO_4)_{14}$ ($0.64 \leq y \leq 0.7$) were synthesized and characterized. The structures of these phosphates were refined using Rietveld analysis. The compound o-$Ca_{19}Cu_2(PO_4)_{14}$ has β-$Ca_3(PO_4)_2$-like structure (Space Group $R3c$, $z = 3$). Compounds r′-$Ca_{19}Cu_2H_{1.42}(PO_4)_{14}$ and r″-$Ca_{19}Cu_{2-y}H_{2.24}(PO_4)_{14}$ ($0.64 \leq y \leq 0.7$) have the whitlockite-like structure (Space Group $R3c$, $z = 3$). The corresponding crystal data are (i) o-$Ca_{19}Cu_2(PO_4)_{14}$: $a = 10.3633(1)$ Å, $c = 37.242(2)$ Å, $V = 3463.8(9)$ Å^3, $R_p = 4.24\%$, $R_{wp} = 5.75\%$; (ii) r′-$Ca_{19}Cu_2H_{1.42}(PO_4)_{14}$: $a = 10.3987(1)$ Å, $c = 37.300(2)$ Å, $V = 3493.0(9)$ Å^3, $R_p = 4.89\%$, $R_{wp} = 6.50\%$; (iii) r″-$Ca_{19}Cu_{2-y}H_{2.24}(PO_4)_{14}$ ($0.64 \leq y \leq 0.7$): $a = 10.3975(1)$ Å, $c = 37.274(2)$ Å, $V = 3489.7(9)$ Å^3, $R_p = 4.57\%$, $R_{wp} = 6.04\%$. Redox reactions in calcium/copper double phosphates were investigated by XRD, DTA, DTG, and IR spectroscopy under hydrogen-containing and oxygen-containing atmospheres. These reactions proceed reversibly in the temperature ranges 753–825 K for the reduction process and 973–1173 K for the oxidation process. The redox cycles can be repeated continuously without destroying the crystal lattice. © 1999 Academic Press
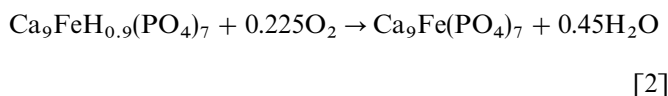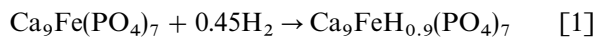
Key Words: phosphates; copper; calcium; redox reactions; crystal structure; Rietveld.

1. INTRODUCTION

Compounds with whitlockite-like structure exhibit interesting properties with potential applications, especially in heterogeneous catalysis (1–3), as luminescent (4, 5) or sensor materials (6), and as intermediators for two-stage oxidation of hydrogen (7). Analysis of the number and dimensions of the polyhedra in the β-$Ca_3(PO_4)_2$ structure (8), which belongs to the whitlockite $Ca_{18.19}Mg_{1.17}Fe_{0.83}H_{1.62}(PO_4)_{14}$ (9), allowed simulation of new compounds $Ca_9R(PO_4)_7$ (R = rare earth, Y, Bi, Sc, Cr, Fe, In) (10, 11), $Ca_{10}M(PO_4)_7$ and $Ca_9MgM(PO_4)_7$ (M = Li, Na, K, Cu) (12, 13), and triple phosphates in $Ca_3(PO_4)_2$–RPO_4–Na_3PO_4

systems (14). The interest of these phases is increased owing to the high degree of chemical, mechanical, and thermal stability provided by the PO_4^{3-} groups. The chemical and thermal stability of whitlockite-like phases promotes reversible redox reactions. Such reactions proceed without the destruction of the crystal lattice, but with a change in the oxidation state of the transition metal.

The redox reactions proceed in the crystal lattice of $Ca_9Fe(PO_4)_7$ (15, 16), $Ca_{18}Na_3Fe(PO_4)_{14}$ (17), and $Ca_{19}Ce(PO_4)_{14}$ (18), avoiding structure destruction. The reduction reaction is accompanied by the incorporation of protons into the crystal lattice, while the oxidation reaction involves their elimination (15–18). The corresponding reactions proceed in accordance with the following schemes (15):

$$Ca_9Fe(PO_4)_7 + 0.45H_2 \rightarrow Ca_9FeH_{0.9}(PO_4)_7 \qquad [1]$$

$$Ca_9FeH_{0.9}(PO_4)_7 + 0.225O_2 \rightarrow Ca_9Fe(PO_4)_7 + 0.45H_2O$$

$$[2]$$

Similar reactions proceed in calcium/copper double phosphate, $Ca_{19}Cu_2(PO_4)_{14}$. The crystal structure of s-$Ca_{19}Cu_2(PO_4)_{14}$ was investigated by us earlier (19). This paper reports the crystal structures and redox characteristics of new calcium copper phosphates synthesized under different conditions as analyzed using XRD, infrared spectroscopy, DTA, TG, DTG measurements, and kinetics of hydrogen absorption.

2. EXPERIMENTAL

Chemical Synthesis

The materials used in this study were synthesized from β-$Ca_3(PO_4)_2$ and $Cu_3(PO_4)_2$ by solid state reaction. Calcium orthophosphate β-$Ca_3(PO_4)_2$ was prepared by sintering a 1:1 stoichiometric ratio of $Ca_2P_2O_7$ and $CaCO_3$ at

973–1173 K for 50–90 h. Calcium pyrophosphate $Ca_2P_2O_7$ was obtained from $CaHPO_4$ by heating at 900–973 K for 7–15 h. Copper phosphate $Cu_3(PO_4)_2$ was prepared by sintering a stoichiometric ratio of CuO and $NH_4H_2PO_4$ at 973–1173 K for 40–80 h. All starting compounds were of analytical grade. The stoichiometric mixture of β-$Ca_3(PO_4)_2$ and $Cu_3(PO_4)_2$ was heated at 973–1173 K for 50–90 h. The solid state reaction was carried out in a platinum crucible under air. The blue product contained the pure s-$Ca_{19}Cu_2(PO_4)_{14}$ phase.

The reaction of hydrogen with $Ca_{19}Cu_2(PO_4)_{14}$ was studied in a setup including a quartz tube reactor and a manometer. A powdered sample of this material was placed in the reactor, heated to the required temperature in an argon flow, and kept at this temperature for the desired time. The temperature was monitored by a Pt–Pt/Rh thermocouple with an accuracy of ± 0.5 K. When the required conditions were achieved, the argon flow was terminated, the reactor was partially evacuated, and a portion of hydrogen was injected through a thick-walled rubber tube with a syringe. The pressure in the reactor was monitored by a water manometer. The reduced sample was then oxidized with atmospheric oxygen at 973 K for 4–6 h. The same sample was used for the successive series of experiments.

For determining and refining structures powder diffraction data were collected using one and the same sample, which was prepared under different conditions:

1. The compound s-$Ca_{19}Cu_2(PO_4)_{14}$ was synthesized from the starting compounds β-$Ca_3(PO_4)_2$ and $Cu_3(PO_4)_2$ by calcining in air at 1173 K for 40 h. The obtained powder was blue. The crystal structure of s-$Ca_{19}Cu_2(PO_4)_{14}$ was investigated earlier (19).

2. The compound s-$Ca_{19}Cu_2(PO_4)_{14}$ was then reduced in a mixture of (84% Ar + 16% H_2) at 753 K for 52 h before being slowly cooled under the same atmosphere. The obtained powder product, named r'-$Ca_{19}Cu_2H_{1.42}(PO_4)_{14}$, was dark gray (see Fig. 1 and Eq. [3] for calculation of $x = 1.42$).

3. The obtained compound r'-$Ca_{19}Cu_2H_{1.42}(PO_4)_{14}$ was also oxidized in air at 973 K for 6 h and slowly cooled. The powder product, named o-$Ca_{19}Cu_2(PO_4)_{14}$, was blue.

4. The compound o-$Ca_{19}Cu_2(PO_4)_{14}$ was reduced in a mixture of (84% Ar + 16% H_2) at 853 K for 58 h, before being slowly cooled under the same atmosphere. The obtained powder, named r''-$Ca_{19}Cu_2H_{2.24}(PO_4)_{14}$, was claret (see Fig. 1 and Eq. [3] for calculation of $x = 2.24$).

Characterization

Powder diffraction data for determination and refinement of the crystal structures were obtained using a SIEMENS D500 powder diffractometer, equipped with a primary SiO_2 monochromator (Cu$K\alpha_1$ radiation, $\lambda = 1.5406$ Å) and a

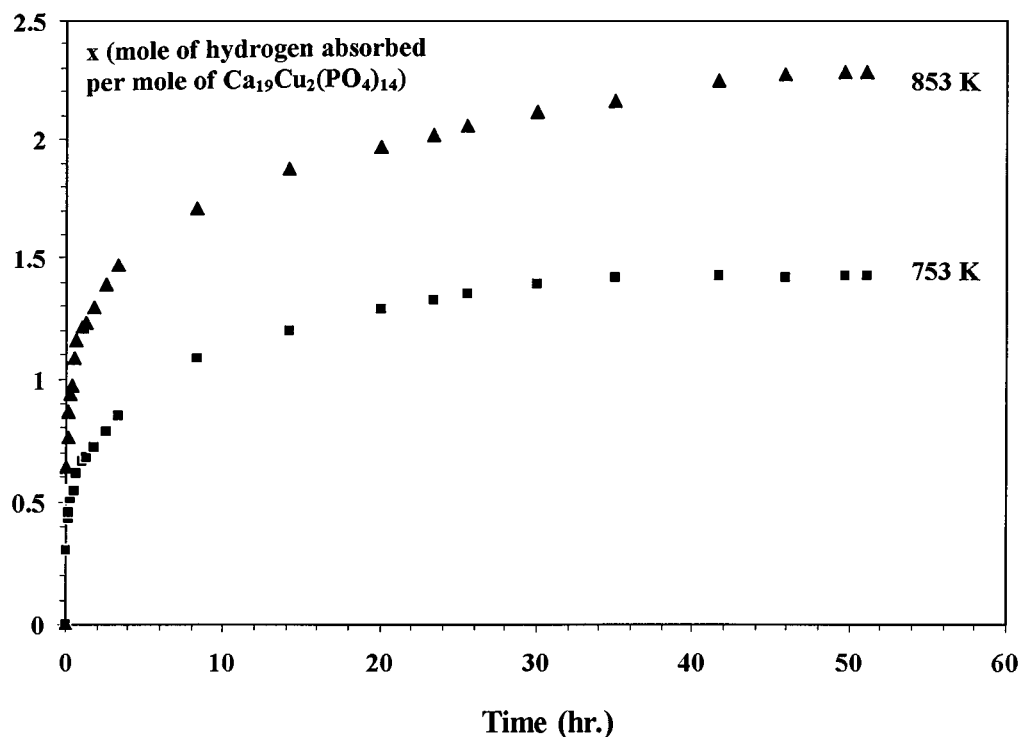**FIG. 1.** Kinetic curves of hydrogen absorption by s- ($T = 753$ K) and o-$Ca_{19}Cu_2(PO_4)_{14}$ ($T = 853$ K). Initial concentration of H_2 was 16% (vol.).

position-sensitive detector (BRAUN). Effective counting time was ca. 30 min per step.

Thermogravimetric and differential thermal measurements were performed between RT and 1200 K, using a derivatograph MOM and Pt crucibles as sample holders (N_2 or air atmosphere); heating rate was $10°$/min.

IR spectra were recorded on a Perkin–Elmer spectrophotometer in the range 400–4000 cm^{-1} using the KBr-pellet technique.

3. RESULTS AND DISCUSSION

Kinetics of Hydrogen Absorption

Figure 1 shows the kinetic curves of the hydrogen reaction with $Ca_{19}Cu_2(PO_4)_{14}$ at two different temperatures. These data indicate that the equilibrium between solid and gas phases is established in the interval of 45–47 h depending on the reaction temperature. The main portion of hydrogen (more than 60%) entered the reducing reaction during the first 6–7 h. Further the reaction proceeds very slowly. At higher temperatures more hydrogen enters the reaction.

The experimental dependence of x (sample reduction degree: see Fig. 1 and Eq. [3]) versus temperature shows that the total compositions of the reduced phases correspond to the formulas r'-$Ca_{19}Cu_2H_{1.42}(PO_4)_{14}$ ($T = 753$ K) and r''-$Ca_{19}Cu_2H_{2.24}(PO_4)_{14}$ ($T = 853$ K). The chemical reactions between hydrogen and the solid phases are expressed by the general equation

$$Ca_{19}Cu_2(PO_4)_{14} + 0.5xH_2 \rightarrow \text{r-}Ca_{19}Cu_2H_x(PO_4)_{14} \quad [3]$$
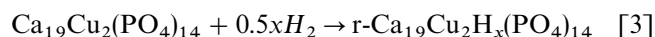
with $x = 1.42$ and $x = 2.24$ for the r'- and r''-phases, respectively.

From the above observations, it is clear that the absoption of hydrogen increases with increasing temperature. Furthermore, the material corresponding to the highest degree of reduction ($x = 2.24$) should involve the presence of Cu^0 according to the $Cu^{2+} \rightarrow Cu^0$ transition.

IR Spectra

IR spectra of samples prepared under different conditions are presented in Fig. 2. Our infrared spectroscopy
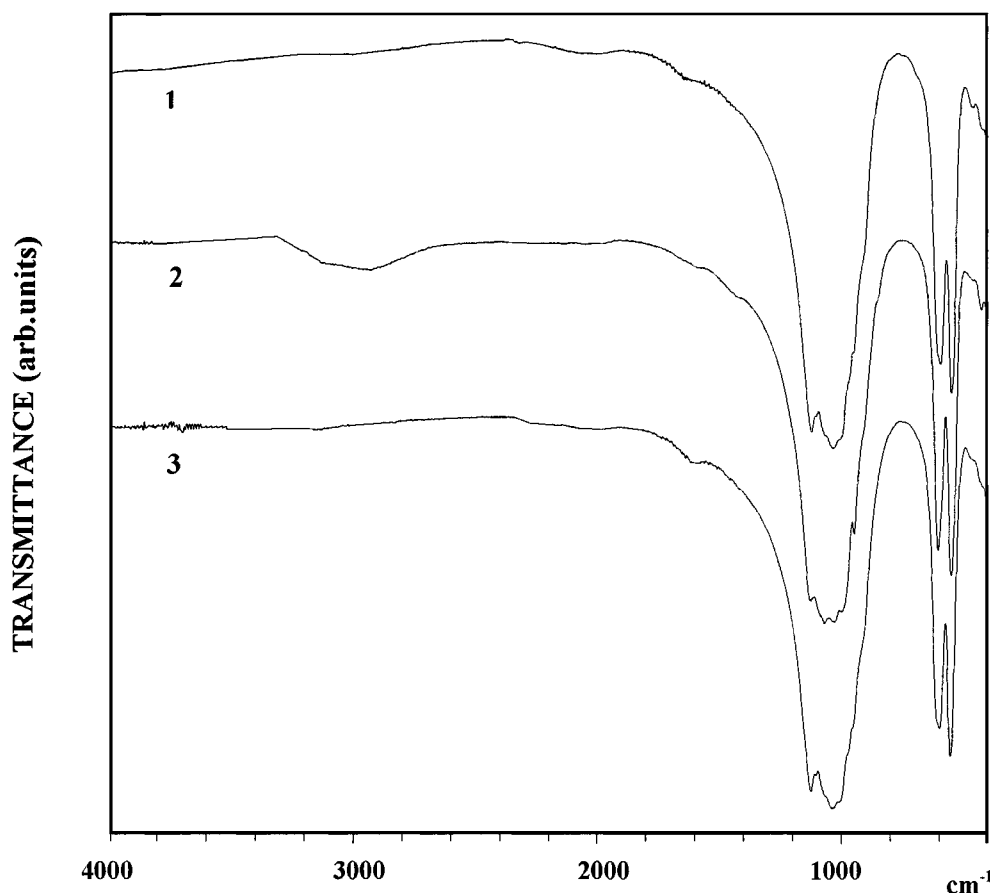
FIG. 2. IR spectra of calcium/copper double phosphates: s-$Ca_{19}Cu_2(PO_4)_{14}$ (1); r'-$Ca_{19}Cu_2H_{1.42}(PO_4)_{14}$ (2); o-$Ca_{19}Cu_2(PO_4)_{14}$ (3). KBr pellet samples were prepared in a dry box.
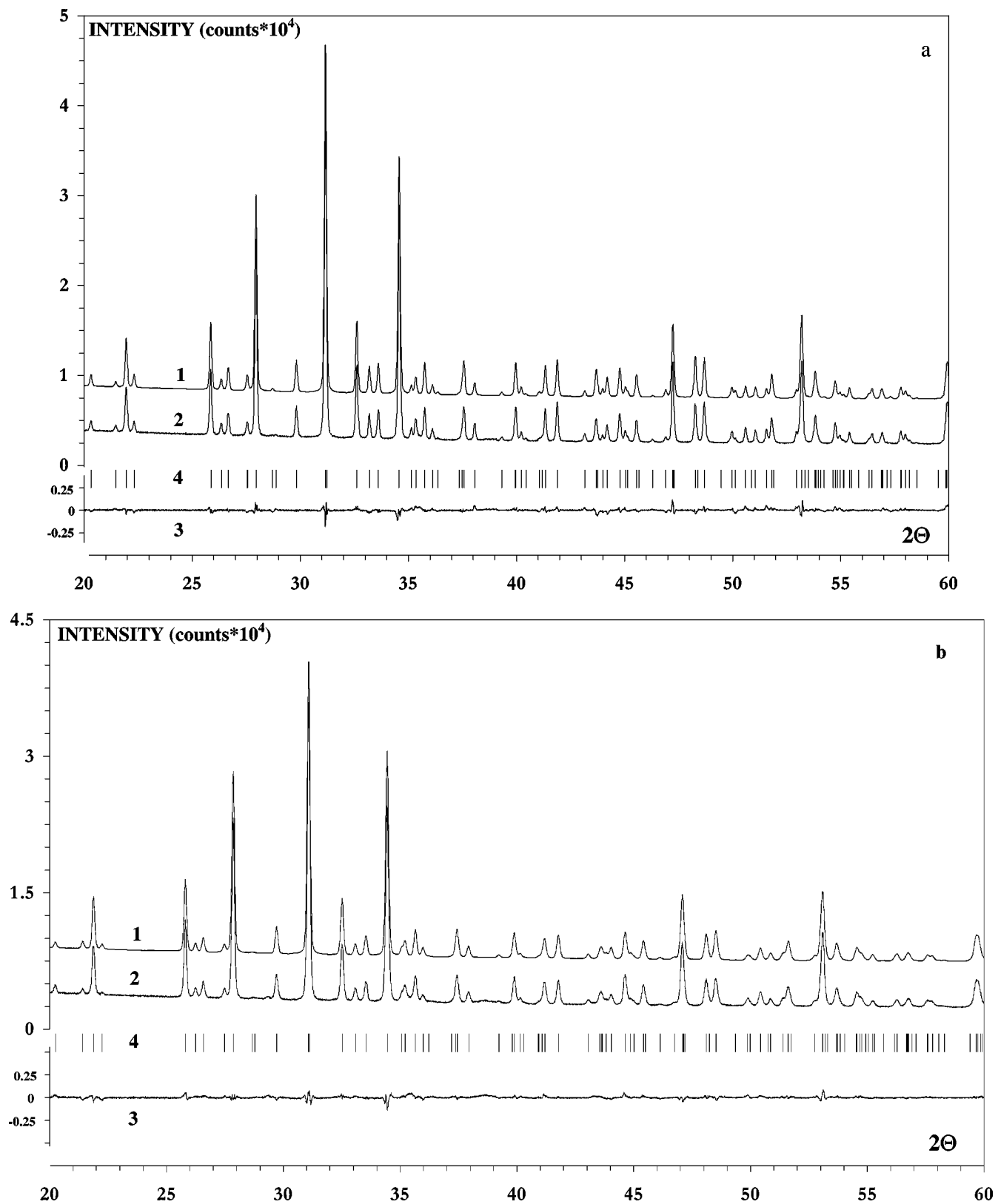
FIG. 3. Final Rietveld calculated (1), observed (2), and difference (3) X-ray powder diffraction patterns of (a) o-$Ca_{19}Cu_2(PO_4)_{14}$; (b) r′-$Ca_{19}Cu_2H_{1.42}(PO_4)_{14}$; (c) total composition sample of r″-$Ca_{19}Cu_2H_{2.24}(PO_4)_{14}$. Bragg reflections of the whitlockite-like structure (4) and metallic copper (5) are given for comparison.

FIG. 3—*Continued*

investigations show that the reduction reaction is accompanied by the introduction of protons into the structure. The proton-related hydroxyls are observed in the region of $\sim 2900 \ cm^{-1}$ fo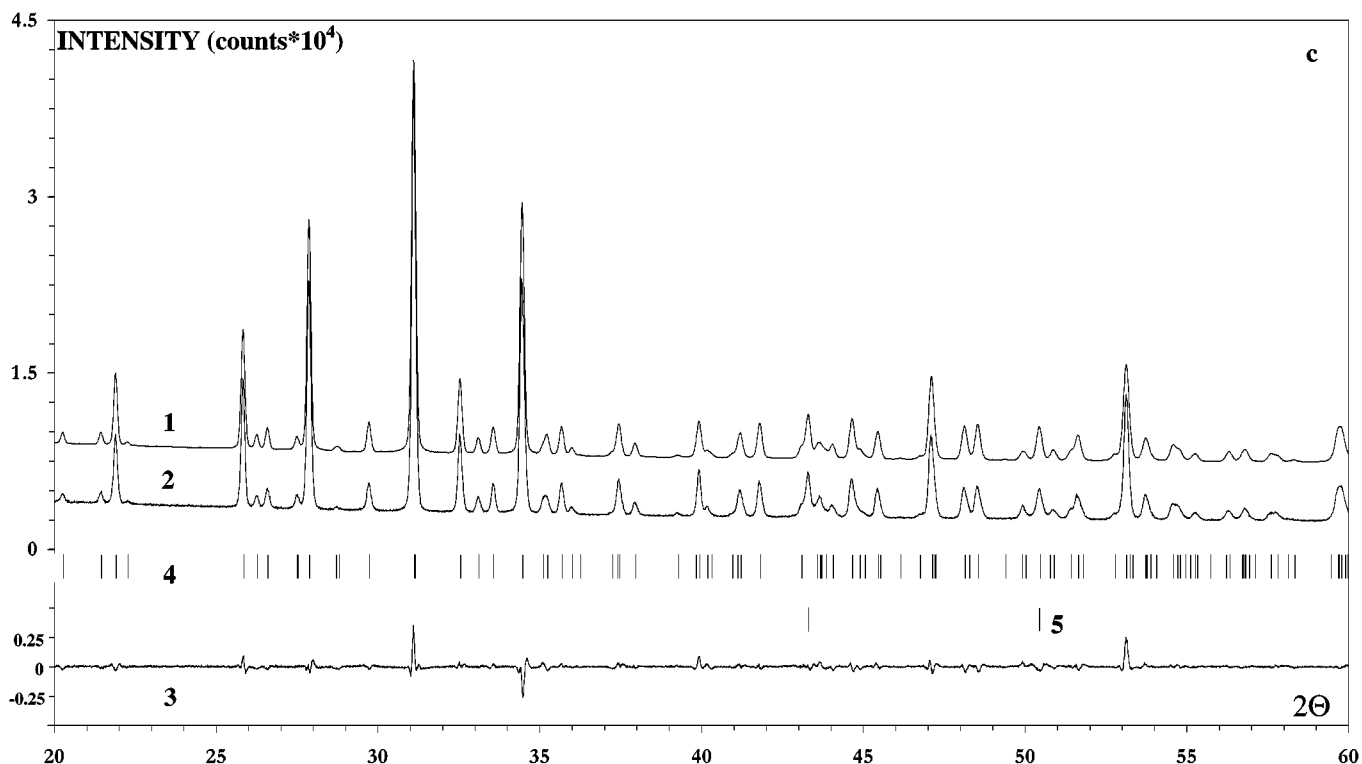r r'-$Ca_{19}Cu_2H_{1.42}(PO_4)_{14}$, but neither observed for s- nor for o-$Ca_{19}Cu_2(PO_4)_{14}$ (Fig. 2). A similar absorption band was also observed for r-$Ca_9FeH_{0.9}(PO_4)_7$ (16). The absorption bands observed in the range 400–1200 cm^{-1} are characteristic of whitlockite-like orthophosphates. The number of absorption bands and the intensity of bands in this region are the same for s- and o-$Ca_{19}Cu_2(PO_4)_{14}$. The IR spectrum of r'-$Ca_{19}Cu_2H_{1.42}(PO_4)_{14}$ is slightly different from the corresponding spectra of s- and o-$Ca_{19}Cu_2(PO_4)_{14}$ (Fig. 2). The IR spectra of r'- and r''-phases do not differ from each other. When s- or o-phases are in contact with air, a band of absorption appears in the region of $\sim 3420 \ cm^{-1}$, which apparently characterises OH^- groups of absorption water.

DTA, TG, and DTG Measurements

Thermogravimetric and differential thermal analyses of s-, o-, and r-phases have been performed to check polymorphism and oxygen stoichiometry changes. In the range from room temperature (RT) to 1200 K for s-, o-, and r-phases, there are neither peaks nor weight change under inert or air atmosphere. The compounds s- and o-$Ca_{19}Cu_2(PO_4)_{14}$

do not change their color in the temperature range from RT to 1200 K. The compositions r-$Ca_{19}Cu_2H_x(PO_4)_{14}$ ($x = 1.42, 2.24$) change their color when they are heated in air ($850 \leq T \leq 1200$ K); however, no change was noticed when they were warmed under N_2 atmosphere ($T \leq 1100$ K). Furthermore, the thermogravimetric and DTA investigations show that oxygen stoichiometry is not variable when the redox reactions proceed in calcium copper double phosphate within the temperature range of 700–825 K.

Structure Determination

The crystal structures of r'-, r''-, and o-phases were refined from X-ray powder data by the Rietveld technique (20) using RIETAN (21) and GSAS (22) programs. The crystal structures of calcium/copper double phosphates were refined using coordinates of atoms in β-$Ca_3(PO_4)_2$ structure (8) as the initial coordinates. Calcium cations are located in $M(1)$, $M(2)$, and $M(3)$ positions. Copper cations occupy the $M(5)$ position, while the $M(4)$ position is occupied by 0.5Ca and 0.5□ (with □ representing a cationic vacancy).

X-ray diffraction patterns of s- (19), r'-, and o-phases are very similar to each other (Figs. 3a, 3b). Although X-ray diffraction patterns of total composition r''-$Ca_{19}Cu_2H_{2.24}$ $(PO_4)_{14}$ are noticeably different from other patterns,
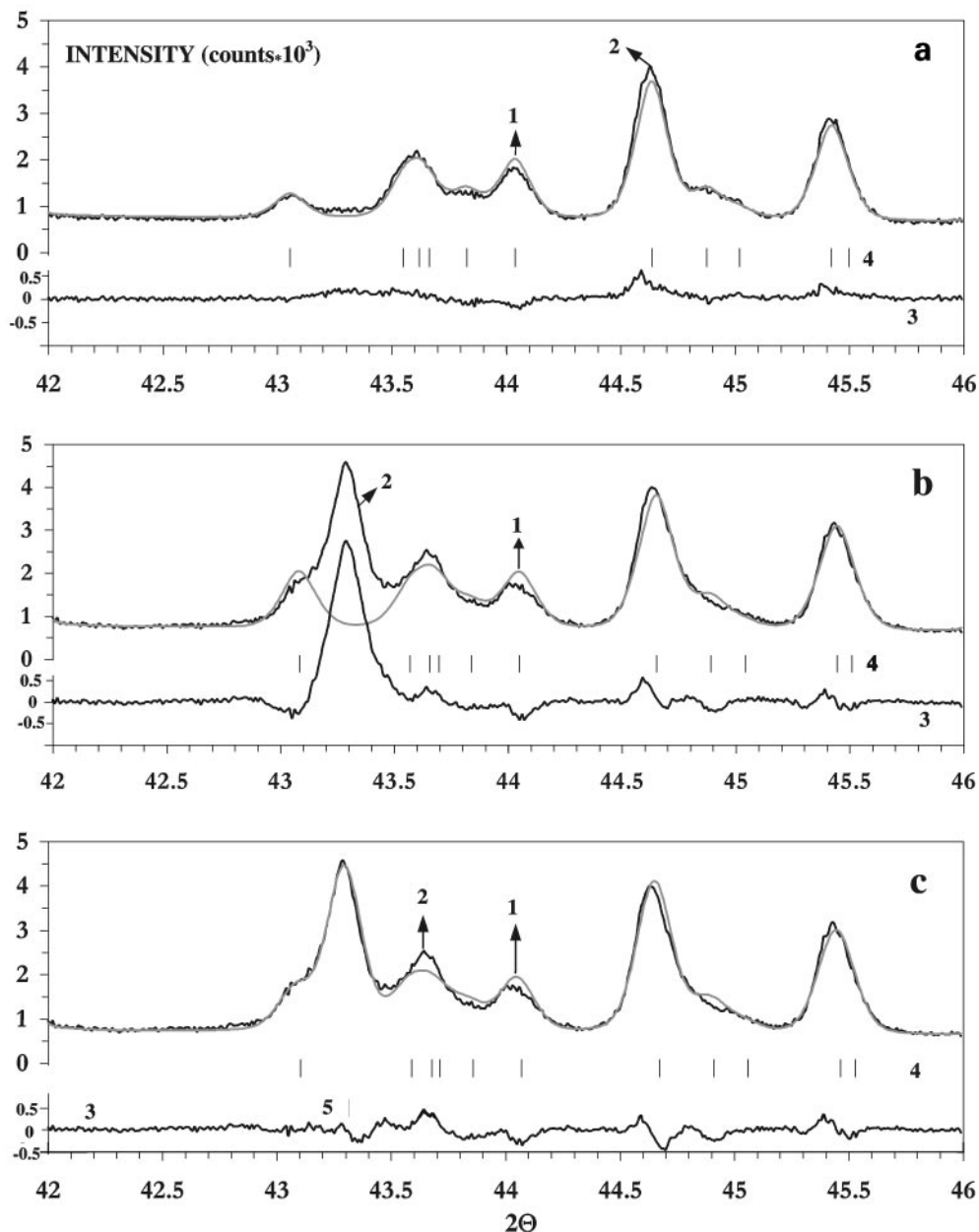
FIG. 4. Fragment of calculated (1), observed (2), and difference (3) X-ray powder diffraction patterns in the intervals $2\Theta = 42–46$ (a, b, c) and $2\Theta = 49–52$ (d, e, f): (a, d) r'-$Ca_{19}Cu_2H_{1.42}(PO_4)_{14}$; (b, e) total composition sample of r''-$Ca_{19}Cu_2H_{2.24}(PO_4)_{14}$ without metallic copper; (c, f) total composition sample of r''-$Ca_{19}Cu_2H_{2.24}(PO_4)_{14}$ with metallic copper. Bragg reflections of the whitlockite-like structure (4) and metallic copper (5) are given for comparison.

both r''- and r'-phases turn into o-phase after oxidation. After the refinement of r'-$Ca_{19}Cu_2H_{1.42}(PO_4)_{14}$ and o-$Ca_{19}Cu_2(PO_4)_{14}$ structures, there were no residual peaks on the Fourier map. For these two structures there is good agreement between the observed and the calculated patterns (Figs. 3a, 3b). After the refinement of the r''-$Ca_{19}Cu_2H_{2.24}(PO_4)_{14}$ structure the Fourier map showed a residual peak. The observed and the calculated patterns do not agree in the regions $2\Theta = 42–46$ and $2\Theta = 49–52$

(Fig. 4). We have assumed that the r''-sample consists of two phases containing both the whitlockite-like and metallic copper phases. As is clear from Fig. 4, the basic lines of metallic copper coincide with the basic lines of the whitlockite-like phase. This is why it is difficult to carry out a correct phase analysis without Rietveld processing of XRD patterns.

With regard to the second phase (metallic copper) the structure refinement of a sample with total composition
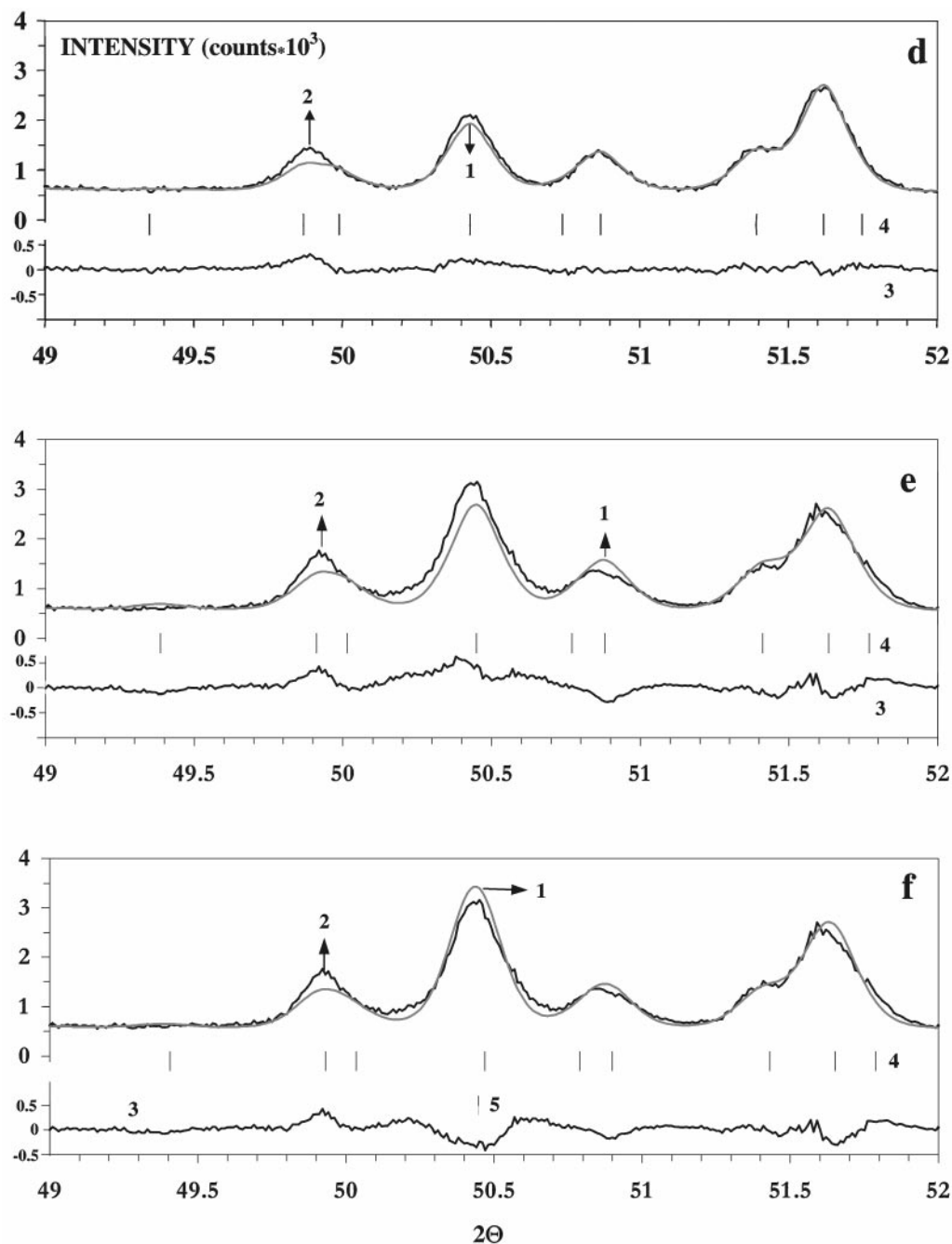
FIG. 4—*Continued*

r''-$Ca_{19}Cu_2H_{2.24}(PO_4)_{14}$ resulted in good agreement between the calculated and the experimental patterns (Figs. 3c, 4c, and 4f). On Fourier maps of $\rho(xyz)$ and $\Delta\rho(xyz)$ there were no residual peaks. While refining isotropic thermal atomic parameters of the whitlockite-type phase in the r''-sample, values of some of them were found to be either very big or negative. In addition, some P–O distances in r'- and

r''-phases were found to be different from the usually observed value.

It is well known that whitlockite-like compounds containing hydrogen have the structure of the synthetic whitlockite $Ca_{18}Mg_2H_2(PO_4)_{14}$ (23), which is similar to β-$Ca_3(PO_4)_2$. They differ by the shift of Ca(3) atoms (~ 0.9 Å) in the polyhedron $Ca(3)O_8$. This is why, to refine the

structures of the r′- and r″-phases, the atomic coordinates of the structure of $Ca_{18}Mg_2H_2(PO_4)_{14}$ (23) were used as the initial model. The position $M(4)$ is vacant in this structure.

The refinement of the location of the calcium cations in $M(4)$ position for both r′-$Ca_{19}Cu_2H_{1.42}(PO_4)_{14}$ and sample total composition of r″-$Ca_{19}Cu_2H_{2.24}(PO_4)_{14}$ has improved the description of two structures. The thermal parameters of calcium and phosphor atoms were then found positive. In the sample total composition of the r″-$Ca_{19}Cu_2H_{2.24}(PO_4)_{14}$ structure the positions $M(5)$ contain $(68\%Cu^{2+} + 32\%Ca^{2+})$, while in the r′-$Ca_{19}Cu_2H_{1.42}(PO_4)_{14}$ structure the same positions are totally (100%) occupied by copper atoms. In the case of a sample with the total composition r″-$Ca_{19}Cu_2H_{2.24}(PO_4)_{14}$ the whitlockite-like phase would have the composition r″-$Ca_{19}Cu_{1.36}H_{2.24}(PO_4)_{14}$. By the Rietveld method it was calculated that the r″-sample, reduced at 853 K, contained 2.0% (wt.) metal copper and 98.0% (wt.) $Ca_{19}Cu_{2-y}H_{2.24}(PO_4)_{14}$. From these data it follows that the whitlockite-like phase has the composition r″-$Ca_{19}Cu_{1.3}H_{2.24}(PO_4)_{14}$. These methods of calculation give an approximately identical composition (within the limits of experimental error) of the whitlockite-like phase, r″-$Ca_{19}Cu_{2-y}H_{2.24}(PO_4)_{14}$ ($0.64 \leq y \leq 0.7$).

It is necessary to note that the refinement of s- and o-$Ca_{19}Cu_2(PO_4)_{14}$ structures in the $Ca_{18}Mg_2H_2(PO_4)_{14}$ model (23) degrades the structural description as against the case when the β-$Ca_3(PO_4)_2$ (8) model is used. Thus, compounds s- and o-$Ca_{19}Cu_2(PO_4)_{14}$ are isostructural to

TABLE 1
Crystallographic Data, Recording Conditions, and Refinement Results of Calcium/Copper Double Phosphates

	r′-phase[a]	o-phase[b]	r″-phase[a]
Space group	$R3c$	$R3c$	$R3c$
2Θ range (°)	10–140	10–120	10–120
Step scan increment (2θ)	0.01	0.01	0.01
I_{max}	33941	38118	37726
Unit cell parameters:			
a (Å),	10.3987(1)	10.3633(1)	10.3975(1)
c (Å),	37.300(2)	37.242(2)	37.274(2)
V (Å³),	3493.0(9)	3463.8(9)	3489.7(9)
Z	3	3	3
Number of reflections	774	534	524
Reliability factors[c]			
R_{WP}	6.50	5.75	6.04
R_P	4.89	4.24	4.57
R_I	3.40	1.76	1.94
R_F	1.42	1.07	1.01
S	2.02	1.88	2.02

Note. o-phase: o-$Ca_{19}Cu_2(PO_4)_{14}$; r′-phase: r′-$Ca_{19}Cu_2H_{1.42}(PO_4)_{14}$; r″-phase: r″-$Ca_{19}Cu_{2-y}H_{2.24}(PO_4)_{14}$ ($0.64 \leq y \leq 0.7$).
[a] Structure refined in the model of synthetic whitlockite, $Ca_{18}Mg_2H_2(PO_4)_{14}$ (23).
[b] Structure refined in the model of β-$Ca_3(PO_4)_2$ (8).
[c] Defined as in (21).

TABLE 2
Fractional Atomic Coordinates and Thermal Parameters for Calcium/Copper Double Phosphates

Atom	Phase	x/a	y/b	z/c	B_{iso}
Ca(1)	r′-	0.7189(3)	0.8460(4)	0.4323(2)	1.06(1)
	o-	0.7259(3)	0.8576(3)	0.4316(1)	0.66
	r″-	0.7217(4)	0.8438(4)	0.4340(1)	0.58(2)
Ca(2)	r′	0.6124(3)	0.8110(4)	0.2324(2)	0.7(1)
	o-	0.6183(2)	0.8226(4)	0.2306(1)	0.66
	r″-	0.6157(3)	0.8110(4)	0.2334(2)	0.81(2)
Ca(3)	r′	0.2041(3)	0.3806(2)	0.3378(2)	1.1(2)
	o-	0.1249(3)	0.2721(2)	0.3252(1)	0.66
	r″-	0.1975(4)	0.3769(3)	0.3387(1)	1.03(2)
Ca(4)[a]	r′	0.0	0.0	0.1791(2)	2.52(5)
Ca(4)[a]	o-	0.0	0.0	0.1819(2)	0.66(2)
Ca(4)[b]	r″-	0.0	0.0	0.1823(5)	2.3(5)
Cu	r′	0.0	0.0	0.0	2.44(2)
Cu	o-	0.0	0.0	0.0	0.96(5)
Cu[c]	r″-	0.0	0.0	0.0	0.96(8)
P(1)	r′	0.0	0.0	0.2569(2)	1.18(2)
	o-	0.0	0.0	0.2639(1)	1.3(1)
	r″-	0.0	0.0	0.2589(2)	2.72(5)
P(2)	r′	0.680(1)	0.860(1)	0.1340(2)	0.81(2)
	o-	0.6844(3)	0.8595(4)	0.1340(1)	0.78(8)
	r″-	0.6823(5)	0.8606(4)	0.1354(1)	1.13(3)
P(3)	r′	0.648(1)	0.837(2)	0.0317(2)	0.26(5)
	o-	0.6515(4)	0.8437(4)	0.0307(1)	0.68(8)
	r″-	0.6499(3)	0.8390(4)	0.0329(2)	0.59(3)
O(11)	r′	0.0	0.0	0.299(1)	2.5(5)
	o-	0.0	0.0	0.3061(3)	0.7
	r″-	0.0	0.0	0.302(2)	1.7(2)
O(12)	r′	−0.022(9)	0.844(7)	0.2424(3)	1.9(2)
	o-	0.0161(7)	0.8675(5)	0.2544(3)	0.7
	r″-	−0.017(7)	0.8527(4)	0.2418(2)	0.2(2)
O(21)	r′	0.726(1)	0.882(1)	0.1738(3)	3.1(1)
	o-	0.734(1)	0.916(1)	0.1736(2)	0.7
	r″-	0.726(1)	0.871(1)	0.1738(2)	1.5(2)
O(22)	r′	0.760(1)	0.777(1)	0.1159(3)	1.0(4)
	o-	0.762(1)	0.778(1)	0.1220(2)	0.7
	r″-	0.755(1)	0.780(1)	0.1167(3)	0.7(2)
O(23)	r′	0.727(1)	0.013(1)	0.1184(3)	1.1(2)
	o-	0.724(1)	0.006(1)	0.1131(2)	0.66
	r″-	0.731(1)	0.018(1)	0.1200(3)	1.2(2)
O(24)	r′	0.515(1)	0.754(1)	0.1286(2)	0.2(1)
	o-	0.513(1)	0.758(1)	0.1318(2)	0.7
	r″-	0.514(1)	0.761(1)	0.1278(2)	1.1(2)
O(31)	r′	0.604(1)	0.936(1)	0.0530(3)	0.3(1)
	o-	0.604(1)	0.955(1)	0.0450(2)	0.7
	r″-	0.601(1)	0.931(1)	0.0530(3)	0.6(2)
O(32)	r′	0.579(1)	0.686(1)	0.0436(3)	0.9(1)
	o-	0.574(1)	0.691(1)	0.0519(2)	0.7
	r″-	0.582(1)	0.684(1)	0.0453(3)	1.0(2)
O(33)	r′	0.817(1)	0.914(1)	0.0383(2)	2.7(1)
	o-	0.825(1)	0.922(1)	0.0403(2)	0.7
	r″-	0.8204(8)	0.914(1)	0.0385(2)	1.3(2)
O(34)	r′	0.6116(9)	0.8419(9)	0.9882(3)	2.3(3)
	o-	0.6243(6)	0.8246(8)	0.9916(2)	0.7
	r″-	0.608(1)	0.8411(8)	0.9894(3)	1.7(2)

Note. o-phase: o-$Ca_{19}Cu_2(PO_4)_{14}$; r′-phase: r′-$Ca_{19}Cu_2H_{1.42}(PO_4)_{14}$; r″-phase: r″-$Ca_{19}Cu_{2-y}H_{2.24}(PO_4)_{14}$ ($0.64 \leq y \leq 0.7$);
[a] One-half of the sites are occupied.
[b] $0.18Ca^{2+} + 0.82\square$ ($\square$-cationic vacancy).
[c] $0.68Cu^{2+} + 0.32Ca^{2+}$.

TABLE 3
Interatomic Distances (Å) and Angles (°) in Calcium/Copper Double Phosphates

Bond	r′-phase	o-phase	r″-phase
Ca(1)–O(12)	2.28(2)	2.51(2)	2.41(3)
–O(22)	2.74(5)	2.92(4)	2.68(5)
–O(23)	2.60(5)	2.48(4)	2.67(5)
–O(24)	2.37(3)	2.53(3)	2.37(5)
–O(24)′	2.60(4)	2.49(5)	2.49(5)
–O(31)	2.30(5)	2.42(3)	2.38(5)
–O(32)	2.46(4)	2.24(4)	2.43(5)
–O(34)	2.31(4)	2.42(3)	2.32(4)
Ca(2)–O(12)	2.48(3)	2.33(3)	2.45(4)
–O(21)	2.42(4)	2.40(4)	2.43(5)
–O(22)	2.33(4)	2.53(4)	2.39(1)
–O(23)	2.41(4)	2.40(4)	2.40(2)
–O(31)	2.53(5)	2.60(4)	2.55(1)
–O(32)	2.84(4)	2.73(4)	2.80(4)
–O(33)	2.46(4)	2.43(4)	2.48(2)
–O(33)′	2.41(3)	2.40(3)	2.45(5)
Ca(3)–O(11)	3.72(1)	2.56(1)	3.66(2)
–O(12)	2.99(2)	2.95(2)	2.98(4)
–O(21)	2.58(5)	2.62(4)	2.55(1)
–O(21′)	2.48(5)		2.54(4)
–O(22)	2.45(4)	2.51(3)	2.52(2)
–O(23)	2.47(5)	2.36(4)	2.39(3)
–O(31)	2.44(4)	2.45(3)	2.43(5)
–O(32)	2.52(4)	2.62(3)	2.48(4)
–O(34)	2.68(5)	2.55(4)	2.67(4)
–O(34)′	3.59(1)	2.54(2)	3.52(3)
Ca(4)–O(12) × 3	2.80(5)	3.08(4)	2.65(1)
–O(21) × 3	2.48(2)	2.46(3)	2.50(2)
–O(22) × 3	3.38(3)	3.28(4)	3.45(2)
Cu–O(24) × 3	2.16(3)	2.08(3)	2.18(3)
–O(33) × 3	2.18(3)	2.18(3)	2.16(2)
O(24)–O(24) × 3	2.83(5)	2.81(5)	2.81(4)
O(33)–O(33) × 3	2.86(4)	2.74(4)	2.80(3)
P(1)–O(11)	1.60(6)	1.58(4)	1.59(3)
–O(12) × 3	1.61(3)	1.51(3)	1.59(4)
⟨P(1)–O⟩	1.60	1.53	1.59
O(11)–O(12) × 3	2.63(5)	2.42(4)	2.66(4)
O(12)–O(12) × 3	2.62(3)	2.72(3)	2.52(2)
O(11)–P(1)–O(12) × 3	109.7(2)	103.5(1)	113.7(2)
O(12)–P(1)–O(12) × 3	109.3(1)	114.8(8)	104.9(2)
⟨O–P(1)–O⟩	109.5	109.1	109.3
P(2)–O(21)	1.54(1)	1.58(4)	1.49(3)
–O(22)	1.62(2)	1.50(5)	1.54(4)
–O(23)	1.52(4)	1.58(3)	1.56(4)
–O(24)	1.52(3)	1.55(3)	1.55(3)
⟨P(2)–O⟩	1.55	1.55	1.54
O(21)–P(2)–O(22)	106.5(2)	107.8(2)	105.8(2)
O(21)–P(2)–O(23)	107.2(1)	102.7(1)	111.6(2)
O(21)–P(2)–O(24)	112.7(1)	110.4(1)	116.2(4)
O(22)–P(2)–O(23)	113.1(3)	118.1(2)	114.7(3)
O(22)–P(2)–O(24)	103.5(2)	111.6(2)	104.6(2)
O(23)–P(2)–O(24)	111.6(1)	106.4(1)	107.2(5)
⟨O–P(2)–O⟩	109.1	109.5	110.0

TABLE 3—*Continued*

Bond	r′-phase	o-phase	r″-phase
P(3)–O(31)	1.54(6)	1.56(4)	1.49(4)
–O(32)	1.44(4)	1.59(3)	1.47(4)
–O(33)	1.54(3)	1.60(3)	1.55(3)
–O(34)	1.67(4)	1.48(3)	1.69(4)
⟨P(3)–O⟩	1.55	1.56	1.55
O(31)–P(3)–O(32)	112.9(2)	112.8(2)	114.3(4)
O(31)–P(3)–O(33)	102.4(2)	104.1(2)	107.2(6)
O(31)–P(3)–O(34)	111.8(2)	108.1(2)	109.8(2)
O(32)–P(3)–O(33)	111.0(1)	106.2(1)	108.9(5)
O(32)–P(3)–O(34)	112.8(1)	111.3(1)	111.8(6)
O(33)–P(3)–O(34)	112.5(2)	110.6(1)	113.3(4)
⟨O–P(3)–O⟩	110.6	108.8	110.9

Note. o-phase: o-$Ca_{19}Cu_2(PO_4)_{14}$; r′-phase: r′-$Ca_{19}Cu_2H_{1.42}(PO_4)_{14}$; r″-phase: r″-$Ca_{19}Cu_{2-y}H_{2.24}(PO_4)_{14}$ ($0.64 \leq y \leq 0.7$).

β-$Ca_3(PO_4)_2$ (8) and r′-$Ca_{19}Cu_2H_{1.42}(PO_4)_{14}$ and r″-$Ca_{19}Cu_{2-y}H_{2.24}(PO_4)_{14}$ ($0.64 \leq y \leq 0.7$) are isostructural to $Ca_{18}Mg_2H_2(PO_4)_{14}$ (23). For these model structure the $\rho(xyz)$ map exhibited only the peaks of the given atoms. The difference Fourier synthesis $\Delta\rho(xyz)$ revealed no pronounced peaks, and the electron density did not exceed $\pm 0.9e^- \times Å^{-3}$. The crystallographic data are summarized in Tables 1–2. Table 3 shows the selected interatomic distances and angles.

The most distorted CuO_6 coordination spheres were observed for the oxidized forms (s- and o-). As a matter of fact, Cu–O distances range from 2.07 to 2.21 Å (19) for the s-phase and from 2.08 to 2.18 Å for the o-phase (Table 3). The environment of Cu cations appears more regular for both reduced phases r′- and r″- with Cu–O values close to 2.16–2.18 Å (Table 3).

It is necessary to note that introduction (exit) of hydrogen ions into the structure of calcium/copper double phosphate is not accompanied by noticeable change of P(1)–O(11) distances, which is characteristic of $Ca_{18.19}Mg_{1.17}Fe_{0.83}H_{1.62}(PO_4)_{14}$ (9), r-$Ca_9FeH_{0.9}(PO_4)_7$ (16), $Ca_{18}Mg_2H_2(PO_4)_{14}$ (23), and $Ca_{18}Mn_2H_2(PO_4)_{14}$ (24). This is why the analysis of P(1)–O(11) distance change does not give enough grounds for defining the "location" of hydrogen ions in the structure.

Redox reactions proceed with noticeable change of the halfwidth of the diffraction peaks (Fig. 5) and their displacements (Fig. 6). However, the displacements of peaks and their changes of halfwidths come back to the initial state during the opposite reactions. The displacements of peaks show that redox reactions are accompanied by small changes of interatomic distances (Table 3). The return of the initial state of halfwidth of peaks (Fig. 5) demonstrates that redox reactions are proceeding without the destruction of the crystal lattice. Otherwise, the values of peak halfwidth would increase after repeated redox cycles. Their increase
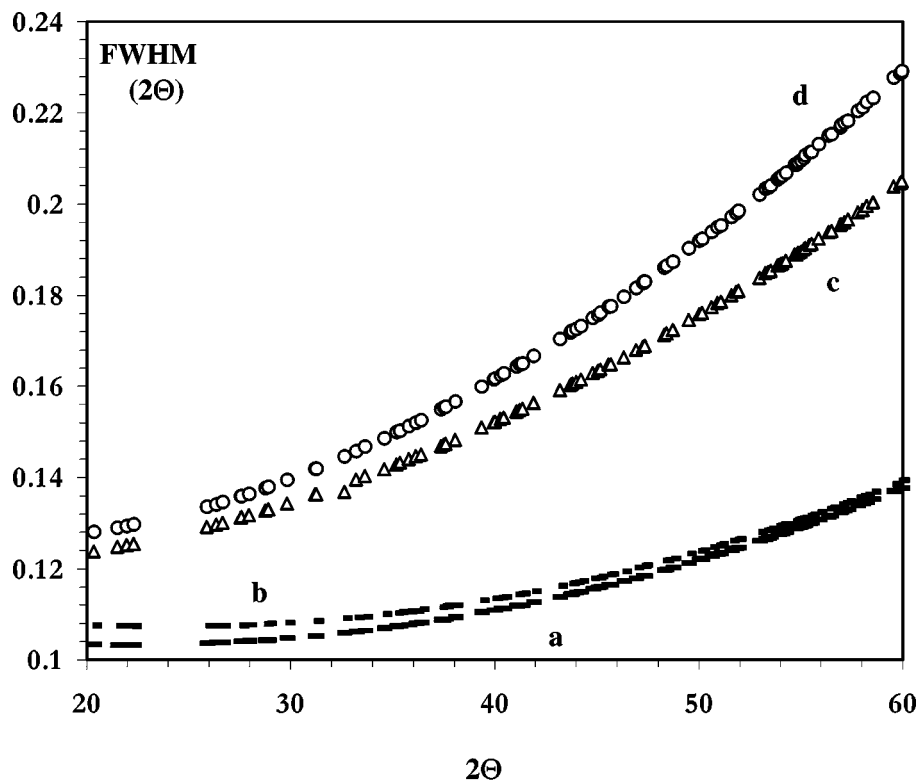
FIG. 5. Halfwidth change of the diffraction peaks in the different structures of calcium/copper phosphates. (a) s-$Ca_{19}Cu_2(PO_4)_{14}$; (b) o-$Ca_{19}Cu_2(PO_4)_{14}$; (c) r'-$Ca_{19}Cu_2H_{1.42}(PO_4)_{14}$; (d) r''-$Ca_{19}Cu_{2-y}H_{2.24}(PO_4)_{14}$ ($0.64 \leq y \leq 0.7$).

during the transition from s-phase to r- and o-phases is caused by microstress in crystals or by the presence of the different oxidized state of the copper cation.
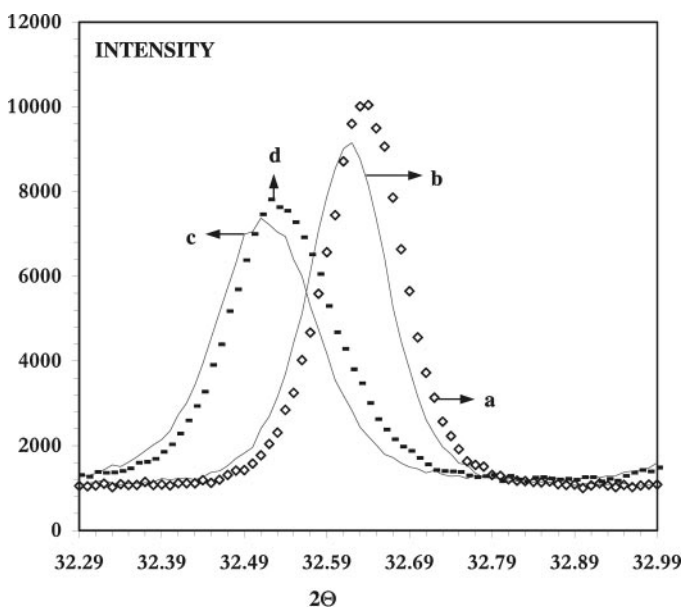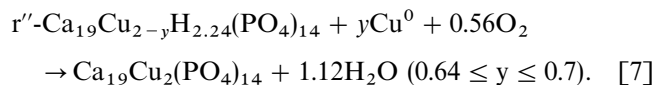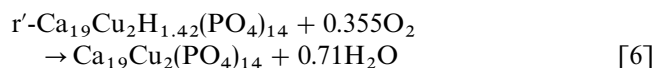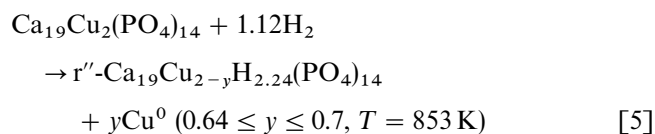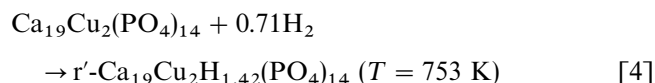

FIG. 6. Halfwidth and position of diffraction reflex (1 2 8) in the structure of calcium/copper phosphates. (a) s-$Ca_{19}Cu_2(PO_4)_{14}$; (b) o-$Ca_{19}Cu_2(PO_4)_{14}$; (c) r'-$Ca_{19}Cu_2H_{1.42}(PO_4)_{14}$; (d) r''-$Ca_{19}Cu_{2-y}H_{2.24}$ $(PO_4)_{14}$ ($0.64 \leq y \leq 0.7$).

From DTA, IR, X-ray, and kinetic experimental data it follows that the redox reactions can be described in the following way:

$$Ca_{19}Cu_2(PO_4)_{14} + 0.71H_2$$
$$\rightarrow r'\text{-}Ca_{19}Cu_2H_{1.42}(PO_4)_{14} \ (T = 753 \text{ K}) \qquad [4]$$

$$Ca_{19}Cu_2(PO_4)_{14} + 1.12H_2$$
$$\rightarrow r''\text{-}Ca_{19}Cu_{2-y}H_{2.24}(PO_4)_{14}$$
$$+ yCu^0 \ (0.64 \leq y \leq 0.7, \ T = 853 \text{ K}) \qquad [5]$$

$$r'\text{-}Ca_{19}Cu_2H_{1.42}(PO_4)_{14} + 0.355O_2$$
$$\rightarrow Ca_{19}Cu_2(PO_4)_{14} + 0.71H_2O \qquad [6]$$

$$r''\text{-}Ca_{19}Cu_{2-y}H_{2.24}(PO_4)_{14} + yCu^0 + 0.56O_2$$
$$\rightarrow Ca_{19}Cu_2(PO_4)_{14} + 1.12H_2O \ (0.64 \leq y \leq 0.7). \quad [7]$$

As follows from the experimental data, up to 825 K redox reactions proceed inside a crystal lattice, where protons can freely enter or exit. At 853 K the reduction reaction proceeds with a partial outflow of copper atoms from the crystal lattice, the formation of a separate phase of metallic copper atoms, and the inflow of protons into the crystal lattice. The oxidation reaction is accompanied by copper

entering the crystal lattice and protons exiting from it. Such reactions do not destroy the whitlockite-like structure. Apparently, only copper atoms from surface microcrystals participate in such reactions.

Thus, the experimental data prove that redox reactions in calcium/copper double phosphates can be repeated and proceed reversibly, avoiding the destruction of the crystal lattice. For example, more than 100 experiments carried out on powder-like polycrystal samples and pellets showed no change in the crystal structure and no destruction of pellets.

ACKNOWLEDGMENTS

REFERENCES

1. A. Legrour, J. Lenzi, and M. Lenzi, *Mater. Chem. Phys.* **38,** 94 (1994).
2. S. Attaly, B. Vigouroux, M. Lenzi, and J. Persia, *J. Catal.* **63,** 456 (1980).
3. M. M. Andrushkevich, G. R. Kotel'nikov, V. V. Molchanov, R. A. Buyanov, and T. V. Strunenkova, *Kinet. Katal.* **21,** 1312 (1980).
4. H. Donker, W. M. A. Smit, and G. Blasse, *J. Electrochem. Soc.* **136,** 3130 (1989).
5. B. I. Lazoryak, T. V. Strunenkova, E. A. Vovk, V. V. Mikhailin, I. N. Shpinkov, A. Yu. Romanenko, and V. N. Schekoldin, *Mater. Res. Bull.* **31,** 665 (1996).
6. B. I. Lazoryak, *in* "Fundamental Study of New Material and Processes in the Substance," p. 54. Moscow State Univ. Press, Moscow, 1994.
7. M. S. Safonov, B. I. Lazoryak, S. B. Pozharskii, and S. B. Dashkov, *Dokl. Acad. Nauk. Russ.* **358,** 663 (1994).
8. B. Dickens, L. W. Schroeder, and W. E. Brown, *J. Solid State Chem.* **10,** 232 (1974).
9. C. Calvo and R. Gopal, *Amer. Mineralog.* **60,** 120 (1975).
10. V. N. Golubev and B. I. Lazoryak, *Inorg. Mater.* (*Sov.*) **35,** 3037 (1991).
11. V. N. Golubev, B. N. Vieting, O. B. Dogadin, B. I. Lazoryak, and R. G. Aziev, *Sov. J. Inorg. Chem.* **35,** 3037 (1990).
12. B. I. Lazoryak, S. V. Khoina, V. N. Golubev, and R. G. Aziev, *Sov. J. Inorg. Chem.* **35,** 1374 (1990).
13. O. V. Yanov, V. A. Morozov, B. N. Vieting, L. N. Ivanov, and B. I. Lazoryak, *Mater. Res. Bull.* **29,** 1307 (1994).
14. B. I. Lazoryak, T. V. Strunenkova, V. N. Golubev, E. A. Vovk, and L. N. Ivanov, *Mater. Res. Bull.* **31,** 207 (1996).
15. B. I. Lazoryak, V. A. Morozov, M. S. Safonov, and S.S. Khasanov, *Mater. Res. Bull.* **30,** 1269 (1995).
16. B. I. Lazoryak, V. A. Morozov, A. A. Belik, S. S. Khasanov, and S. Sh. Shekhtman, *J. Solid State Chem.* **122,** 15 (1996).
17. T. V. Strunenkova, V. A. Morozov, S. S. Khasanov, K. V. Pokholok, A. N. Zhdanova, and B. I. Lazoryak, *Crystallogr. Reports* (*Russ.*) **42,** 64 (1997).
18. B. I. Lazoryak, R. Salmon, C. Parent, P. Hagenmuller, B. N. Vieting, and A. B. Yaroslavzev, *Vestn. Mosk. Univ. Ser. 2. Khim.* **31,** 406 (1990).
19. N. Khan, V. A. Morozov, S. S. Khasanov, and B. I. Lazoryak, *Mater. Res. Bull.* **32,** 1211 (1997).
20. H. M. Rietveld, *Acta Crystallogr.* **22,** 151 (1967).
21. F. Izumi, *in* "The Rietveld Method" (R. A. Young, Ed.), p. 236. Oxford Univ. Press, Oxford, 1993.
22. A. C. Larson and R. B. Von Dreel, "Generalized Crystal Structure Analysis System (GSAS)." Los Alamos Report LAUR 86-748, Los Alamos, 1981.
23. R. Gopal, C. Calvo, J. Ito, and W. K. Sabine, *Can. J. Chem.* **52,** 1155 (1974).
24. E. Kostiner and J. R. Rea, *Acta Crystallogr.* **32,** 250 (1976).